19

Investigation of the effect of spatial dispersion in a metal shell of a non-spherical magnetoplasmonic nanoparticle

© Yu.A. Eremin, V.V. Lopushenko ¶

Moscow State University,
119991 Moscow, Russia

¶ e-mail: lopushnk@cs.msu.ru

Received June 22, 2022
Revised August 08, 2022
Accepted August 08, 2022

Based on the method of discrete sources, the effect of spatial dispersion in the metal shell of a magnetoplasmonic nanoparticle on the absorption of electromagnetic energy is studied. Hybrid particle is composed of a magnetic core Fe_3O_4 or Fe_2O_3 and a golden shell. The influence of the elongation of spheroidal particles on the level of energy absorption is considered. It is shown that taking into account the spatial dispersion in the shell leads to a decrease in the absorption cross section to 30% and is accompanied by a shift of the plasmon resonance to the short-wavelength region down to 25 nm. It is found that averaging the absorption cross section over the directions of propagation of external excitation and polarizations entails a threefold decrease in the level of absorbed energy.

Keywords: discrete source method, plasmon resonance, spatial dispersion, generalized nonlocal response theory.

DOI: 10.21883/EOS.2022.10.54873.3849-22

Introduction

Nanoplasmonics is a developing area of nanophotonics, in which the processes of the influence of radiation on the collective oscillations of electrons inside nanostructures are studied. The properties of nanoplasmonic structures are largely determined by the resonance phenomena that arise in them. Depending on the material, size and shape of structures, the resonance can be located in a wide range: from ultraviolet to far infrared. Nanoplasmonic structures make it possible to overcome the Rayleigh limit of light diffraction due to the concentration of the optical field near the surface of the structure — at distances of the order of several nanometers from it. This phenomenon has many applications both in the field of fundamental research and modern industrial technologies [1,2].

Plasmonic nanoparticles of various structures with unique optical properties are used in the development of new technologies in many branches of science and industry. „Core-shell" nanoparticles are a special class of nanoparticles consisting of an inner core surrounded by an outer shell. As a result, layered nanoparticles have properties inherent in their individual components. As a result, „core-shell" particles acquire increased functionality and high potential for their use in a wide range of applications, including biomedical, pharmaceutical, catalysis, electronics, and optics [3,4].

Magnetoplasmonic layered nanoparticles consisting of a magnetic core (Fe_3O_4 or Fe_2O_3) and a gold shell , proved to be a very effective tool for targeted pharma drug delivery and therapy [3,5]. Let's note the main advantages of magnetoplasmonic particles.

1. The magnetic core allows you to manipulate particles (due to the magnetic field), directing them in a given direction and controlling their concentration, thereby reducing the potential risk of damage to healthy tissues.

2. High refraction index makes it possible to synthesize stable core and shell configurations in a wide range of sizes. The gold shell protects the core from corrosion, providing biocompatibility with the tissues of a living organism, and the presence of plasmon resonance (PR) in the gold layer provides additional opportunities for imaging and medical treatment of neoformations.

3. By changing the core size, its material, the shell thickness, as well as the shape (elongation) of the particles, it is possible to achieve the maximum absorption energy in the transparency window of biological tissues (range 700−900 nm of the electromagnetic spectrum), where the absorption by the surrounding biological tissue is minimal.

Exotic nanoparticles with controlled sizes, morphology and composition are currently being designed and manufactured for various applications [6,7]. In the presence of a metallic shell, it becomes necessary to take into account the resonant collective oscillations of free electrons, which cause a localized surface PR. Resonances lead to a sharp and strong enhancement of the absorption and scattering of optical radiation. Part of the electromagnetic energy absorbed by the plasmon shell is converted into heat due to the Joule effect. Thus, the illuminated nanoparticle become like a point source of heat. Introduced into human tissue, it, illuminated at the frequency of PR, causes burnout and destruction of the affected cell. For example, layered Fe_3O_4@Au nanoparticles can significantly enhance absorption in the near transparency window of biological

tissues [8], which allows them to be used in photothermal cancer cell therapy [9,10].

The description of PR phenomena in nanostructures is based on the application of the fundamental laws of physics, namely, on the use of Maxwell's theory. However, the method of describing the properties of nanostructures within the framework of classical electrodynamics and using the macroscopic functions of a plasmonic metal has its limitations. Problems arise when the respective length scales approach the sub-nanometer range, in which the characteristic mean free paths of an electron or a Fermi wave predominate. In this case, the local connections between the displacement and the electric field are broken and a spatial dispersion of the metal appears [11,12]. To study such effects, one can use a purely quantum approach based on solving the Schrödinger equation for an electron cloud in a metal [13]. However, this approach becomes computationally cumbersome for particles larger than ten nanometers, as well as for metals with a high density of free charge carriers, such as noble metals [14]. In the latter case, the most acceptable is the use of quasi-classical models, which make it possible to study plasmon effects while remaining within the framework of the Maxwell system. One of such approaches, which allows taking into account the spatial dispersion (SD) of a plasmonic metal, is the theory of generalized nonlocal response (GNR) [15,16]. This theory, in particular, makes it possible to study the optical characteristics of plasmonic nanoparticles of non-spherical geometry, taking into account SD [17].

There are a number of methods that allow one to study the optical characteristics of hybrid particles, taking into account the spatial dispersion of materials. The main part consists of approaches related to the study of particles with spherical symmetry [18,19]. In the case of violation of spherical symmetry or deviation of the shape of surfaces from spherical, numerical-analytical approaches are used, such as the T-matrix method, which makes it possible to analyze layered non-spherical particles taking into account the SD in the layer [20,21]. For inhomogeneous arbitrarily shaped scatters, the available numerical results are in most cases obtained using either the finite difference-time domain method (FDTD) [22] or the finite element method (FEM) included in the COMSOL Multiphysics package [23]. It should be noted that numerical methods have certain limitations associated with the minimum discretization of the inhomogeneity, which is about 0.2 nm. However, such discretization may not be sufficient for a thorough study of the characteristics of the near field.

Issues related to the necessary conditions for taking into account the SD of layered spherical particles were studied in detail in the Ph.D. thesis [19]. It was found there, in particular, that with an increase in the thickness of the gold shell above 4ṅm, the influence of the SD on the shift of the PR in the frequency domain becomes imperceptible in a wide range of changes in the diameters of the dielectric core. This is consistent with the experimental results reported in the same work, which demonstrate the general trend that the smaller the size of the plasmonic metal, the greater the deviation of the results from the classical local case.

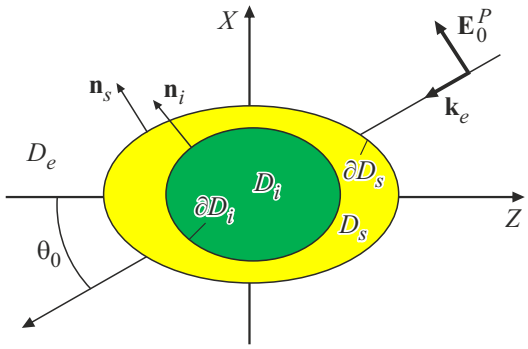

Figure 1. Diffraction of a plane wave by a spheroidal layered particle.

In the present work, on the basis of the discrete source method (DSM), the effect of SD arising in a thin gold shell of magnetoplasmonic particles, is studied. The conditions under which the maximum of the absorption cross section falls within the transparency window of biological tissues are determined. As a result of simulating, it was found that taking into account the SD in the shell leads to a decrease in the amplitude of the absorption cross section to 30% and a shift of the maximum to the short-wavelength region to 25 nm.

1. Boundary problem statement

Let's now write the statement of the boundary value problem for the diffraction of a plane electromagnetic (EM) linearly polarized wave $\mathbf{E}_0, \mathbf{H}_0$ propagating at an angle $\pi - \theta_0$ with respect to the symmetry axis OZ, on a layered axisymmetric particle (Fig. 1).

The boundary value problem of diffraction using the theory of GNR can be written in the following form.

1. Helmholtz equations for the total field $\mathbf{E}_i$ in D_i and the scattered field $\mathbf{E}_e$ in D_e

$$\Delta \mathbf{E}_{i,e}(M) + k_{i,e}^2 \mathbf{E}_{i,e}(M) = 0, \quad M \in D_{i,e}. \tag{1}$$

2. Helmholtz equations for the total field $\mathbf{E}_s = \mathbf{E}_{sT} + \mathbf{E}_{sL}$ inside the plasmonic film D_s, which consists of classical transverse irrotational $\mathbf{E}_{sT}$ ($\mathrm{div}\mathbf{E}_{sT} = 0$) and longitudinal $\mathbf{E}_{sL}$ ($\mathrm{rot}\mathbf{E}_{sL} = 0$) fields

$$\Delta \mathbf{E}_{sT}(M) + k_s^2 \mathbf{E}_{sT}(M) = 0,$$

$$\Delta \mathbf{E}_{sL}(M) + k_L^2 \mathbf{E}_{sL}(M) = 0, \qquad M \in D_s. \tag{2}$$

2. Boundary conditions for fields on media interfaces $\partial D_{i,s}$, including additional boundary conditions for normal field components,

$$\mathbf{n}_i \times \mathbf{E}_i(P) = \mathbf{n}_i \times \mathbf{E}_s(P),$$

$$\mathbf{n}_i \times \mathrm{rot}\mathbf{E}_i(P) = \mathbf{n}_i \times \mathrm{rot}\mathbf{E}_s(P), \qquad P \in \partial D_i,$$

$$\varepsilon_i \mathbf{n}_i \mathbf{E}_i(P) = \varepsilon_L \mathbf{n}_i \mathbf{E}_s(P), \tag{3}$$

$$\mathbf{n}_s \times (\mathbf{E}_s(P) - \mathbf{E}_e(P)) = \mathbf{n}_s \times \mathbf{E}_0(P),$$

$$\mathbf{n}_s \times (\mathrm{rot}\mathbf{E}_s(P) - \mathrm{rot}\mathbf{E}_e(P)) = \mathbf{n}_s \times \mathbf{H}_0(P), \qquad P \in \partial D_s,$$

$$\varepsilon_L \mathbf{n}_s \mathbf{E}_s(P) = \varepsilon_e \mathbf{n}_s (\mathbf{E}_e(P) + \mathbf{E}_0(P)). \tag{4}$$

3. Silver–Muller radiation conditions at infinity for a scattered field $\mathbf{E}_e$.

Here $\mathbf{E}_{i,s}, \mathbf{H}_{i,s}$ are fields in $D_{i,s}$, $\mathbf{n}_{i,s}$ are unit normals to $\partial D_{s,i}$, $k^2_{i,s,e} = k^2 \varepsilon_{i,s,e}$, $k^2_L = \varepsilon_s/\xi^2$, $k = \frac{2\pi}{\lambda}$, $\varepsilon_L = \varepsilon_s - \frac{\omega_p^2}{(j\gamma\omega - \omega^2)}$, $\xi^2 = \frac{\varepsilon(\beta^2 + D(\gamma + j\omega))}{(\omega^2 - j\gamma\omega)}$, ε_s is complex permittivity of gold, ω is frequency of light waves, ω_p is plasma frequency of gold, γ are damping coefficients, β — hydrodynamic velocity $\beta^2 = 0.6 v_F^2$, v_F is Fermi velocity, D is electron diffusion coefficient [16]. Wherein, the characteristics of the medium are chosen so that the time dependence $\exp\{j\omega t\}$ satisfies $\mathrm{Im}\varepsilon_e = 0$, $\mathrm{Im}\varepsilon_{i,s} \le 0$, $\mathrm{Im}\varepsilon_L \le 0$. We will assume that stated boundary problem (1)–(4) with radiation conditions has a unique classical solution.

It should be emphasized that SD occurs only in metals with a high concentration of free charges, such as the noble metals gold, silver, and platinum. Therefore, both in the external medium and in the magnetic core, there is no longitudinal field.

2. Discrete sources method

Since the principle scheme of the DSM for constructing an approximate solution has been repeatedly stated [17,24,25], we will focus only on the fundamental stages of this construction.

1. It is considered P/S-polarization of a plane wave propagating at an angle $\pi - \theta_0$ to the axis of symmetry of the geometry of the problem OZ. Approximate solution is constructed separately for P- and S-polarizations. Discrete sources (DS) for transverse and longitudinal fields are located on the symmetry axis OZ. Distributed multipoles of lower order [25] are supposed to be the basis of representation for fields.

2. The transverse EM field is built on the basis of vector potentials, the Cartesian components of which satisfy the Helmholtz equation (1), and the longitudinal field is plotted on the basis of a scalar potential that satisfies the equation $\Delta\Psi_s(M) + k_L^2 \Psi_s(M) = 0$.

3. The fields constructed in this way satisfy all the conditions of the original boundary value problem, except for the conjugation conditions on the media interfaces. The DS amplitudes are determined from the satisfaction of these conditions on the basis of the generalized collocation method [25]. Since the approximate solution is a finite sum of harmonics with respect to the azimuthal variable φ, satisfying the boundary conditions on the $\partial D_{i,s}$ surfaces reduces to successive matching of the Fourier harmonics on the generators of these surfaces.

4. As before [24], the accuracy of the approximate solution is controlled by calculating the residual of the boundary conditions on the surfaces $\partial D_{i,s}$ using the plane wave field $\mathbf{E}_0$, $\mathbf{H}_0$.

5. After all the DS amplitudes are determined, the components of the scattering diagram are easily calculated, which take the following form for the P-polarization:

$$F_\theta^P(\theta, \varphi) = jk_e \sum_{m=0}^{M} (j \sin\theta)^m \cos(m+1)\varphi \times \sum_{n=1}^{N_e^m} (p_{mn}^e \cos\theta + q_{nm}^e) \exp(-jk_e z_n^e \cos\theta) - jk_e \sin\theta \sum_{n=1}^{N_e^0} r_n^e \exp\{-jk_e z_n^e \cos\theta\},$$

$$F_\theta^P(\theta, \varphi) = -jk_e \sum_{m=0}^{M} (j \sin\theta)^m \sin(m+1)\varphi \times \sum_{n=1}^{N_e^m} (p_{mn}^e + q_{nm}^e \cos\theta) \exp(-jk_e z_n^e \cos\theta) \tag{5}$$

and for the S-polarization

$$F_\theta^S(\vartheta, \varphi) = jk_e \sum_{m=0}^{M} (j \sin\theta)^m \sin(m+1)\varphi \times \sum_{n=1}^{N_e^m} (p_{mn}^e \cos\theta - q_{nm}^e) \exp(-jk_e z_n^e \cos\theta),$$

$$F_\varphi^S(\vartheta, \varphi) = jk_e \sum_{m=0}^{M} (j \sin\theta)^m \cos(m+1)\varphi \times \sum_{n=1}^{N_e^m} (p_{mn}^e \cos\theta - q_{nm}^e) \exp(-jk_e z_n^e \cos\theta) + jk_e \sin\theta \sum_{n=1}^{N_e^0} r_n^e \exp -jk_e z_n^e \cos\theta. \tag{6}$$

Here p_{mn}, q_{mn}, r_n are DS amplitudes for different Fourier harmonics (m) and different DS positions (n), and z_n^e are coordinates of the DS corresponding to the scattered field.

Since the main goal is to calculate the absorption cross section, we will use the optical theorem [26] to determine it, namely, the relation of the form

$$\sigma_{\mathrm{ext}}(\theta_0, \lambda) = \sigma_{\mathrm{scs}}(\theta_0, \lambda) + \sigma_{\mathrm{abs}}(\theta_0, \lambda).$$

Here σ_{ext} is the extinction cross section, σ_{scs} is the scattering cross section, σ_{abs} — is the absorption cross section. In our case, the scattering cross section is defined as

$$\sigma_{\mathrm{scs}}^{P,S}(\theta_0, \lambda) = \int_\Omega DSC^{P,S}(\theta_0, \theta, \varphi) d\Omega, \tag{7}$$

where is the differential scattering cross section is

$$DSC^{P,S}(\theta_0, \theta, \varphi) = |F_\theta^{P,S}(\theta_0, \theta, \varphi)|^2 + |F_\varphi^{P,S}(\theta_0, \theta, \varphi)|^2.$$

In addition, we will calculate the extinction cross sections for P- and S-polarizations, whichcan be calculated as [25]

$$\sigma_{\text{ext}}^{P}(\theta_0, \lambda) = -\frac{4\pi}{k_e}\text{Im}F_\theta^P(\pi - \theta_0, \pi);$$

$$\sigma_{\text{ext}}^{S}(\theta_0, \lambda) = \frac{4\pi}{k_e}\text{Im}F_\varphi^s(\pi - \theta_0, \pi); \qquad (8)$$

Summarizing the above, we will determine the absorption cross section as follows:

$$\sigma_{\text{abs}}(\theta_0, \lambda) = \sigma_{\text{ext}}(\theta_0, \lambda) - \sigma_{\text{scs}}(\theta_0, \lambda). \qquad (9)$$

It is easy to see that integration over φ in formula (7), due to (5), (6), is carried out in an analytical form and it remains to calculate the integral over θ for each Fourier (m) -harmonics.

3. Numerical results

Let's pass to consideration of numerical results. Since hybrid nanoparticles with an average size of 10–20 nm are used in practice, and the characteristic thickness of the gold film is only 2-5 nm [27,28], we will consider precisely this range of layered nanoparticle sizes. Let's choose the core diameter $D = 12$ nm. Let's study spherical and spheroidal particles as the most commonly used, while deforming the particle will keep the core volume as fixed. Layered spheroidal particles are also known as core-shell nanorice [29,30]. As the material of the magnetic core, we will consider Fe_3O_4 and Fe_2O_3 [31], and as the material of the shell we will consider the gold. When performing calculations, we will take into account the frequency dispersion of the refraction index of the core $n_i = \sqrt{\varepsilon_i}$, taking the required values from the database [32], and for gold $n_s = \sqrt{\varepsilon_s}$ from the [33]. Quantum parameters of gold (Au), corresponding to the theory of GNR, we take in accordance with [16]:

$$\hbar\omega_p = 9.02\,\text{eV}, \qquad \hbar\gamma = 0.071\,\text{eV},$$

$$v_F = 1.39\frac{10^{12}\,\mu\text{m}}{\text{s}}, \quad D = 8.62\frac{10^{8}\,\mu\text{m}^2}{\text{s}}.$$

We will assume that the particle is in a medium with a refraction index $n_e = \sqrt{\varepsilon_e}$, and $n_e = 1.33$ (water). In the paper [34], spherical magnetoplasmonic nanoparticles were considered, consisting of a magnetic core and a gold shell with a SD arising in it. As a result of the simulation, the following was established.

1. An increase in the particle core diameter or a decrease in the shell thickness leads to a shift of the PR maximum to the long wavelength region.

2. The use of Fe_2O_3 in the core instead of Fe_3O_4 leads to an increase in the PR amplitude, simultaneously shifting the PR to the infrared wavelength range.

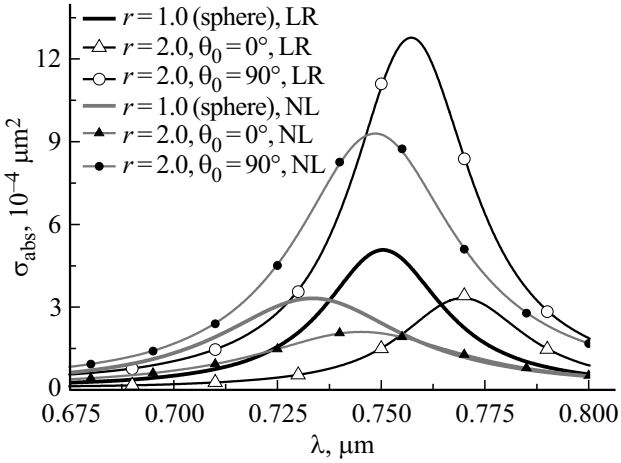

Figure 2. Influence of SP on the absorption cross section for a sphere and a spheroid with the ratio of the axes $r = 2$ at different angles of incidence. The curves obtained in the absence (LR) and presence (NL) of SD are shown.

In this study, we will consider elongated spheroidal particles (nanorice), which are used in practice [30]. The advantage of such particles is that the magnetic core of the elongated spheroidal particles allows them to be oriented in a given direction using a constant magnetic field. When the nanoparticles are oriented, one can use a polarized optical source, for example, with P polarization, to optimize the excitation of the local PR absorption cross section, thereby enhancing the photothermal heating process while using more moderate optical powers [30].

Let us carry out a comparative analysis of the behavior of the absorption cross section for a sphere and a spheroid with the ratio of the axes $r = 2$, consisting of the core Fe_2O_3, covered with a gold shell 2 nm thick. Fig. 2 shows the results for various angles of incidence of a P-polarized plane wave ($\theta_0 = 0°$, $90°$). It can be seen from the results that, in the case of taking into account the SD (NL curves), a spherical particle and a spheroid with axial incidence of the wave $\theta_0 = 0°$ demonstrate a shift of the PR up to 25 nm with a decrease in its amplitude compared to case without taking into account SD (curves LR). For a spheroid $r = 2$ at an angle of incidence $\theta_0 = 90°$ and P-polarization (vector $\mathbf{E}_0$ is parallel to the major axis), the PR amplitude increases by a factor of 3 compared to the spherical case.

Fig. 3 shows the curves of absorption cross section versus wavelength for $r = 2$ spheroids with two different shell thicknesses at an angle of incidence $\theta_0 = 90°$ and P-polarization at absence (LR lines) and presence of SD (NL lines). It can be seen that an increase in the thickness of the shell entails an increase in the PR amplitude with a simultaneous shift of the PR by 75 nm to the region of short waves and an exit from the transparency region of biomaterials.

A similar behavior can be observed in Fig. 4 for the Fe_3O_4 core. In this case, the PR peaks turn out to be shifted to the region of short wavelengths by about the same 75 nm.

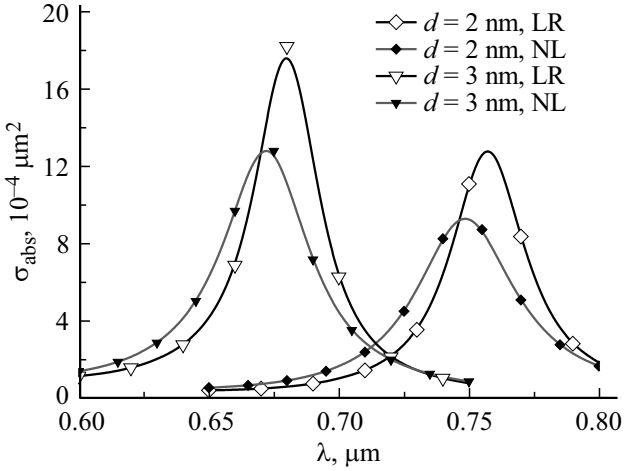

Figure 3. Absorption cross section for a spheroidal particle with axis ratio $r = 2$ and core Fe_2O_3 for different thicknesses of the gold shell. The cases of absence (LR) and presence (NL) of SD are considered.

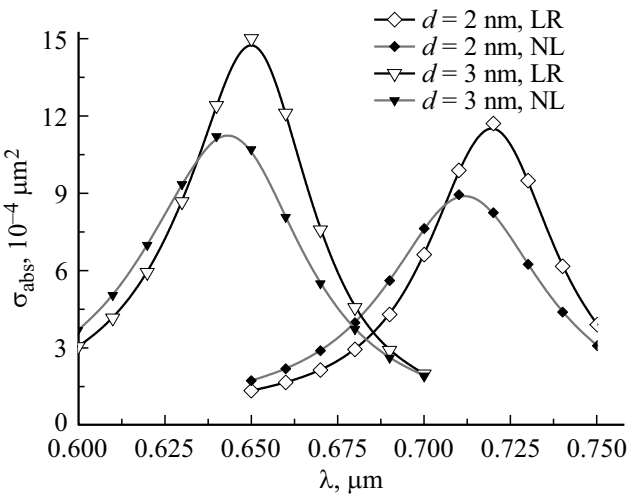

Figure 4. Absorption cross section for a spheroidal particle with axis ratio $r = 2$ and core Fe_3O_4 for different thicknesses of the gold shell. The results obtained in the absence (LR) and presence (NL) SD.

Fig. 5 shows the dependences of the absorption cross section of EM radiation on the elongation of a spheroid with a Fe_2O_3 core and a gold shell 2 nm thick at an angle of incidence of a P-polarized wave $\theta_0 = 90°$. As expected, an increase in elongation while maintaining the volume of the nucleus entails a shift in the PR to the region of transparency of biological tissues with a simultaneous increase in the amplitude of the PR. In all the above cases, the effect of SD (curves NL) turns out to be very significant. Thus, the decrease in the PR amplitude exceeds 25% with a shift to the region of short waves of about 15 nm.

The results of Fig. 6 demonstrate the effect of the environment on the position and amplitude of the PR in a spheroidal particle with a Fe_2O_3 core and a gold shell 2 nm thick at an incidence angle P-polarized wave $\theta_0 = 90°$. Water $n_e = 1.33$, medulla $n_e = 1.36$ and female breast biomaterial $n_e = 1.405$ [35] were chosen. As is clear from the results, an increase in tissue density entails a shift in the PR to the depth of the transparency region of biological tissues. As in the previous cases, taking into account the SD in the shell is accompanied by a decrease in the PR to 30% with a slight shift to the region of short waves.

Fig. 7 is devoted to studying the influence of particle orientation (Fe_2O_3 core and $d = 2$ nm shell) with respect to the direction of external excitation propagation. For this, the absorption cross section for the P polarization is averaged over the angles of incidence of the wave in the range $\theta_0 \in (0°, 90°)$. As can be seen from the above results, this entails a decrease in absorbance by about 42%. Additional averaging over polarizations leads to an additional decrease in the PR value. In this case, the total decrease in

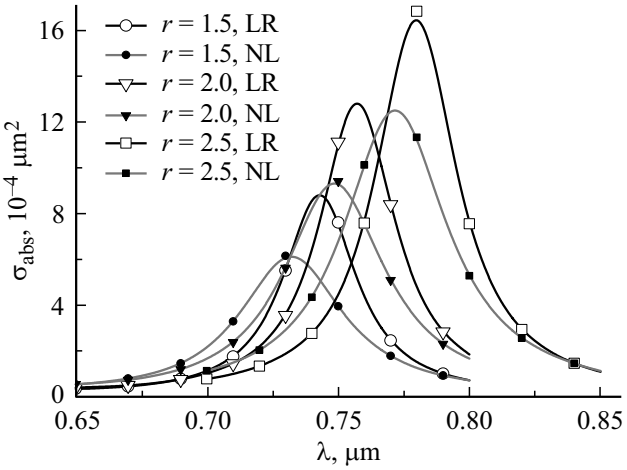

Figure 5. Influence of spheroid elongation on the absorption cross section without taking into account (LR) and taking into account (NL) SD.

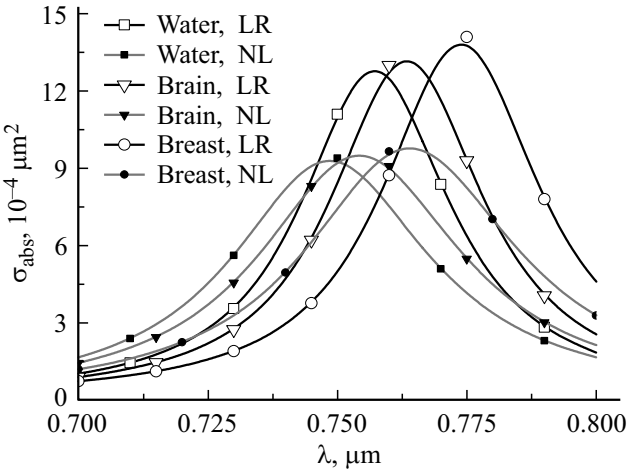

Figure 6. Influence of the environment on the position and amplitude of the PR in a spheroid with the ratio of the axes $r = 2$ without taking into account (LR) and taking into account (NL) SD.

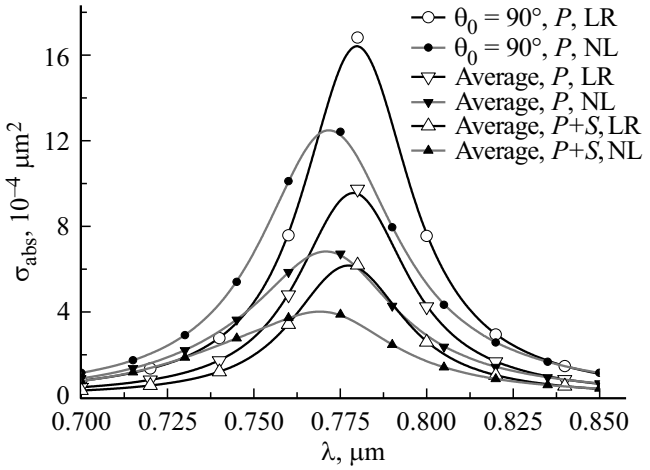

Figure 7. Change in the absorption cross section of the spheroid ($r = 2.5$) when averaging over the angles of incidence and polarizations with and without (NL) SD.

amplitude is about 67%. This circumstance demonstrates the importance of taking into account the orientation of particles with respect to the direction of external excitation.

Conclusion

In conclusion, we formulate the main results of the work.

1. DSM was adapted to study the problem of absorption of electromagnetic energy by a hybrid non-spherical particle, composed of a magnetic core and a gold shell, taking into account the SD of gold in the framework of the theory of GNR.

2. It has been convincingly shown that an increase in the elongation of a particle parallel to the direction of polarization of the external field, while maintaining the volume of the particle core, makes it possible to significantly increase the amount of absorbed energy and simultaneously shift the absorption maximum to the region of transparency of biological tissues.

3. Accounting for SD leads to a decrease in the absorbed energy to 30% with a shift to the region of short waves by a value of about 25 nm.

4. Averaging the absorption cross section over the angles of incidence and polarizations entails a decrease in the absorbed energy by a factor of three. This circumstance demonstrates the importance of particle orientation and makes it possible, when using a P-polarized radiation source, to optimize the process of photothermal heating at moderate optical powers, contributing to the preservation of healthy tissues and their rapid recovery.

Summarizing the above, we note that taking into account SD is necessary to develop an optimal strategy for the practical application of magnetoplasmonic layered particles in the implementation of photothermal heating of oncological formations in order to use moderate optical powers and save surrounding healthy tissues.

Funding

The study was supported by a grant from the Russian Science Foundation № 22-21-00110, https://rscf.ru/project/22-21-00110/

Conflict of interest

The authors declare that they have no conflict of interest.

References

[1] J.W.M. Chon, K. Iniewski. *Nanoplasmonics. Advanced Device Applications* (CRC Press, Boca Raton, 2018). ISBN: 9781138072633

[2] G. Barbillon. Photonics, **9** (112), 1 (2022). DOI: 10.3390/books978-3-0365-3704-7

[3] G. Brennan, S. Bergamino, M. Pescio, S.A.M. Tofail, C. Silien. Nanomaterials, **10** (12), 2424 (2020). DOI: 10.3390/nano10122424

[4] McK. Smith, M. McKeague, M.C. Derosa. MethodsX, **6**, 333 (2019). DOI: 10.1016/j.mex.2019.02.006

[5] H-V. Tran, N. Ngo, R. Medhi, P. Srinoi, T. Liu, S. Rittikulsittichai, T.R. Lee. Materials, **15** (2), 503 (2022). DOI: 10.3390/ma15020503

[6] S. Cherukulappurath. *Fundamentals and Properties of Multifunctional Nanomaterials*, ed. by S. Thomas, N. Kalarikkal, A.R. Abraham (Elsevier, Amsterdam, 2021), ch. 13. DOI: 10.1016/B978-0-12-822352-9.00002-X

[7] Z. Fattahi, A.Y. Khosroushahi, M. Hasanzadeh. Biomedicine & Pharmacotherapy, **132**, 110850 (2020). DOI: 10.1016/j.biopha.2020.110850

[8] M. Hadded, A. Hmima, T. Maurer, A. Chehaidar, J. Plain. Optical Materials, **114**, 110946 (2021). DOI: 10.1016/j.optmat.2021.110946

[9] E. Alphandéry. Acta Biomaterialia, **124**, 50 (2021). DOI: 10.1016/J.ACTBIO.2021.01.028

[10] I. Mukha, O. Chepurna, N. Vityuk, A. Khodko, L. Storozhuk, V. Dzhagan, D.R.T. Zahn, V. Ntziachristos, A. Chmyrov, T.Y. Ohulchanskyy. Nanomaterials, **11**(5), 1113 (2021). DOI: 10.3390/nano11051113

[11] P.E. Stamatopoulou, Ch. Tserkezis. Optical Materials Express, **12**(5), 1869 (2022). DOI: 10.1364/OME.456407

[12] Y. Huang, L. Gao. J. Phys. Chem. C, **118**(51), 30170 (2014). DOI: 10.1021/jp508289z

[13] M. Barbry, P. Koval, F. Marchesin, R. Esteban, A.G. Borisov, J. Aizpurua, D. Sánchez-Portal. Nano Lett., **15**(5), 3410 (2015). DOI: 10.1021/acs.nanolett.5b00759

[14] M. Kupresak, X. Zheng, A.E. Vandenbosch, V.V. Moshchalkov. Adv. Theory and Simul., **3**(1), 1900172 (2020). DOI: 10.1002/adts.201900172

[15] N.A. Mortensen, S. Raza, M. Wubs, T. Søndergaard, S.I. Bozhevolnyi. Nature Communications, **5**, 3809 (2014). DOI: 10.1038/ncomms4809

[16] M. Wubs, N.A. Mortensen. *Quantum Plasmonics*, ed. by S.I. Bozhevolnyi, L. Martin-Moreno, F. Garcia-Vidal (Springer, Berlin/Heidelberg, 2017), p. 279. DOI: 10.1007/978-3-319-45820-5_12

[17] Yu.A.Eremin Opt. i spektr., **128** (9), 1388 (2021) (in Russian). DOI: 10.21883/OS.2020.09.49881.141-20
[Yu.A. Eremin. Opt. Spectr., **128**, 1500 (2021). DOI: 10.1134/S0030400X20090088]
[18] C. David, F.J. García de Abajo. J. Phys. Chem. C, **115**(40), 19470 (2011). DOI: 10.1021/jp204261u
[19] C. David. *Nonlocal and Collective Phenomenain the Plasmons of Metallic Nanostructures* (Doctoral Thesis, Universidad Aut onoma de Madrid, 2014)
[20] Y. Huang, L. Gao. J. Phys. Chem. C, **118**(51), 30170 (2014). DOI: 10.1021/jp508289z
[21] A. Doicu, Yu. Eremin, T. Wriedt. J. Quantitative Spectroscopy and Radiative Transfer, **254**, 107196 (2020). DOI: 10.1016/j.jqsrt.2020.107196
[22] J.M. McMahon, S.K. Gray, G.C. Schatz. Phys. Rev. B, **82**(3), 035423 (2010). DOI: 10.1103/PhysRevB.82.035423
[23] *COMSOL — Software for Multiphysics Simulation* [Electronic source]. URL: https://www.comsol.com/
[24] Yu.A. Eremin, A.G. Sveshnikov. Zhurn. vychisl. matem. i matem. fiz., **61**(4), 34 (2021) (in Russian). DOI: 10.31857/S0044466921040049 [Yu.A. Eremin, A.G. Sveshnikov. Comput. Math. and Math. Phys., **61**(4), 564 (2021). DOI: 10.1134/S0965542521040047].
[25] Yu.A. Eremin. Opt. i spektr., **129** (8), 1079 (2021) (in Russian). DOI: 10.21883/OS.2021.08.51205.1872-21
[Yu.A. Eremin. Opt. Spectrosc., **129**, 1095 (2021). DOI: 10.1134/S0030400X21080087].
[26] R.G. Newton. *Scattering Theory of Waves and Particles* (McGraw Hill, 1966).
[27] Z. Izadiyan, K. Shameli, M. Miyake, S-Y. Teow, S-C. Peh, S.E. Mohamad, S.H.M. Taib. Mater. Sci. Eng.: C, **96**, 51 (2019). DOI: 10.1016/j.msec.2018.11.008
[28] T. Dasri, A. Chingsungnoen. J. Magnet. Magnet. Mat., **456**, 368 (2018). DOI: 10.1016/j.jmmm.2018.02.066
[29] T.T. Nguyen, F. Mammeri, S. Ammar. Nanomaterials, **8**(3), 149 (2018). DOI: 10.3390/nano8030149
[30] C.M. García-Rosas, L.A. Medina, P. Lopez, N. Large, A. Reyes-Coronado. J. Nanoparticle Research, **23**, 144 (2021). DOI: 10.1007/s11051-021-05261-x
[31] T. Mahmoudi-Badiki, E. Alipour, H. Hamishehkar, S.M. Golabi. J. Electroanal. Chem., **788**, 210 (2017). DOI: 10.1016/j.jelechem.2017.02.011
[32] *Refractive index database* [Electronic source]. URL: https://refractiveindex.info
[33] P.B. Johnson, R.W. Christy. Phys. Rev. B, **6**, 4370 (1972). DOI: 10.1103/PhysRevB.6.4370
[34] Yu.A. Eremin, V.V. Lopushenko. Nanomaterials, **11**, 3297 (2021). DOI: 10.3390/nano11123297
[35] R. Khan, B. Gul, S. Khan, H. Nisar, I. Ahmad. Photodiagnosis Photodyn. Ther., **33**, 102192 (2021). DOI: 10.1016/j.pdpdt.2021.102192